Guided-Mode Resonance Gratings for Intermediate Band Quantum Dot Solar Cells

Farid Elsehrawy[1], Tapio Niemi[2], and Federica Cappelluti[1,*]

[1] *Department of Electronics and Telecommunications, Politecnico di Torino, Torino, 10129, Italy*
[2] *Laboratory of Photonics, Tampere University of Technology, P.O. Box 692, FI-33101 Tampere, Finland*
[*] *federica.cappelluti@polito.it*

Abstract: Quantum dot solar cells require very high absorption of the second low-energy photon to operate in the intermediate band regime. We study guided-mode resonance backside gratings demonstrating strong enhancement of intraband optical transitions.

OCIS codes: 040.5350 Photovoltaic; 050.1950 Diffraction gratings; 050.6624 Subwavelength structures

1. Introduction

Efficiency enhancement of solar cells through the use of intermediate band (IB) materials exploits the sequential absorption of two sub-bandgap photons to achieve large photocurrent and high voltage at the same time [1, 2]. The sequential two-photon absorption requires the introduction in the semiconductor forbidden band gap of an energy level or band which supports strong optical transitions from and to the valence band (VB) and conduction band (CB), respectively, while being electrically isolated from them. Quantum dots (QDs) are well suited as an IB material as they form three-dimensional potential wells that provide bound states fully isolated from the continuum bands owing to their zero-dimensional density of states [2]. Strong interband and intraband optical absorption is needed [1] to make QD solar cells operate in the IB regime and reach high efficiency, but from the practical standpoint the QD material effective absorption is limited by the relatively low QD density and low number of QD layers that can be used in the solar cell without compromising the crystal quality. Taking advantage of a thin-film configuration, novel photon management techniques applied to QD solar cells may overcome such limitation [3]. Moreover, thin-film solar cells utilizing QDs are very promising for space applications due to their impressive weight/output power ratio and improved electrical performance [4, 5]. We have previously demonstrated QD photocurrent enhancement in QD thin-film solar cells fabricated by epitaxial lift-off [6]. In this work, we investigate the use of guided-mode resonances (GMR) in thin-film cells [7] patterned with a bi-periodic sub-wavelength grating to enhance the long-wavelength intraband transition. In addition to providing a remarkable increase of the intraband absorption, such a grating acts as diffraction grating at the QD interband transition wavelengths, yielding increased cell absorbance in a wide spectral range.

2. Device Design

The active region of the cell (Fig. 1 (a), (b)) is made of a stack of InAs/GaAs QD layers with overall thickness of 150 nm, embedded within two GaAs layers of 300 nm and 200 nm, respectively. The primary VB - IB transition of the QD material is set to 1.13 eV, and the IB - CB (second low energy photon) transition to 270 meV. The QD optical model for the interband wavelength range was calculated in [8]. The absorption coefficient of the IB - CB transition (α_{IC}) is a subject of theoretical and experimental research, with reported values ranging from few tens to thousands of cm^{-1}. Here, we consider a constant value of 200 cm^{-1} at $\lambda = 4.6\,\mu$m $\pm 0.3\,\mu$m, taken from experimental data of InAs/GaAs QD layers with similar in-plane QD density [9]. In order to independently optimize both anti-reflection and GMR effects, the grating is placed on the back-side, as shown in Fig. 1 (b), and is patterned onto the bottom AlInP layer, which also acts as a back surface field layer. The grating is terminated by a conformal, planarizing polymer layer and a planar Ag mirror to achieve the highest possible reflectivity while preventing parasitic electrical losses and optical loss in the mirror. A dual-layer antireflection coating is used.

The planar layers on top of the grating make a slab waveguiding structure, with supported modes characterized by the effective indexes shown in Fig. 1 (c), calculated according to the slab waveguiding theory. The resonant field enhancement is realized by the GMR grating when a phase matching condition occurs between the evanescent diffracted waves excited by the grating and the waveguides modes supported by the waveguiding structure [7]. Under the hypothesis of weak index modulation, such condition is fullfilled for normal incidence when $\Lambda = m\lambda/n_{eff}$, Λ being the

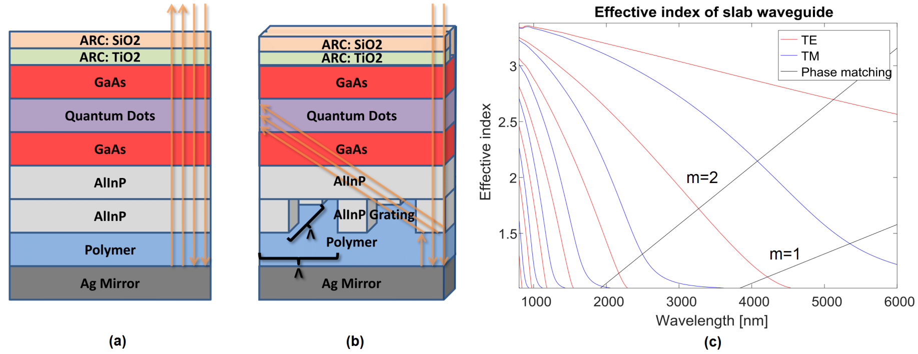

Fig. 1. (a) Reference planar structure and (b) structure terminated by the GMR three-dimensional cubic grating with period=Λ. The layer thicknesses are: 110 nm - SiO_2, 55 nm - TiO_2, 300 nm - GaAs, 150 nm - QD, 200 nm - GaAs, 82 nm - AlInP, 1200 nm - AlInP grating layer, 250 nm - polymer (n=1.55). (c) Effective refractive index of the guided modes as a function of the wavelength, with phase matching conditions for the first (m=1) and second (m=2) orders for a grating with Λ=3.8μm.

grating period, m the diffraction order, λ the incident wavelength, and n_{eff} the effective index of a guided mode. Thus, a suitable grating period is first chosen on the basis of the approximate resonances identified according to Fig. 1 (c). Grating optimization is then based on full electromagnetic simulations. Here, cubic grating structures were simulated using the rigorous coupled-wave analysis (RCWA) method. Optimization - aimed at maximizing the absorbance in the QD photoactive region at the second photon absorption wavelength ($\lambda = 4.6\,\mu$m) - was carried out in terms of period and aspect ratio, by using a fixed duty cycle of 0.5.

3. Results

Fig. 2 (a), (b) show the electric field amplitude and absorbed photon density at 4.6$\,\mu$m of the GMR structure and the reference planar structure, for a grating with optimized period $\Lambda = 3.8\,\mu$m and depth $d = 1.2\,\mu$m demonstrating significant field waveguiding and absorption enhancement in the quantum dot layers. The absorbance in the GaAs and QD regions at short and long wavelengths is reported in Fig. 3 (a) and (b), respectively, for the GMR and reference planar solar cells. The GMR cell shows a remarkable increase of absorbance at the second photon wavelength (Fig. 3 (b)) with respect to the planar one. Based on a simple Lambert-Beer model of the QD stack, the effective optical path length of the 150 nm thick QD stack - or equivalently its effective absorption coefficient - is enhanced by a factor larger than 350. Thus, the material α_{IC} of 200 cm^{-1} turns into a real absorption of 7×10^4 cm^{-1}. Notably, the GMR provides somewhat improved light trapping in the interband QD region ($\lambda = 0.895 - 1.2\,\mu$m, Fig. 3 (a)), whose associated photocurrent increases from 0.509 mA/cm^2 in the planar structure to 1.063 mA/cm^2 in the GMR structure. Finally, Fig. 3 (c) demonstrates the achievable GMR enhancement, defined as the ratio of the absorbance at 4.6 μm of the GMR cell and of the reference planar cell, as a function of the QD intraband optical coefficient. Even for α_{IC} of 1000 cm^{-1}, the absorbance enhancement is as high as 50. This strong enhancement is expected to make the InAs/GaAs QDSC achieve efficiency higher than single-gap GaAs cells even at low concentration [3]. Finally, the structure and approach investigated in this work find important application in intraband quantum-dot infrared detectors.

4. Acknowledgements

The authors wish to acknowledge Prof. Mircea Guina and Timo Aho, with the Laboratory of Photonics at Tampere University of Technology, for useful discussions. The research was supported by the European Union's Horizon 2020 research and innovation program, under Grant Agreement 687253 – TFQD, http://tfqd.eu and by the COST Action MP1406 "Multiscale in modelling and validation for solar photovoltaics" (MultiscaleSolar).

References

1. Y. Okada, N. J. Ekins-Daukes, T. Kita, R. Tamaki, M. Yoshida, A. Pusch, O. Hess, C. C. Phillips, D. J. Farrell, K. Yoshida, N. Ahsan, Y. Shoji, T. Sogabe, and J.-F. Guillemoles, "Intermediate band solar cells: Recent progress and future directions," Applied Physics Reviews **2**, 021,302 (2015).

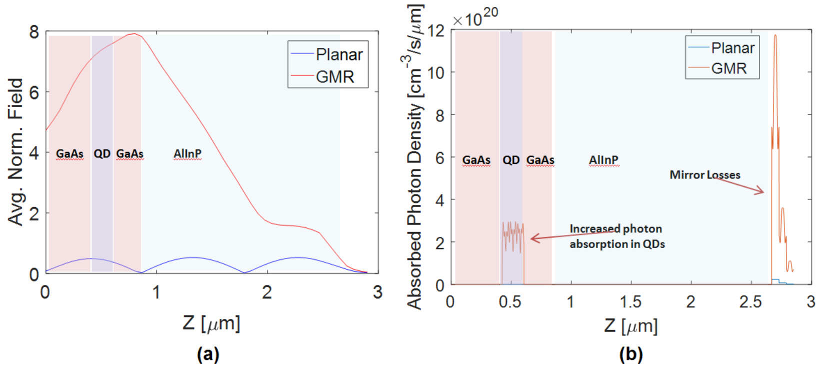

Fig. 2. (a) Average electric field amplitude and (b) average spatial absorbed photon density at $\lambda = 4.6\,\mu$m. The spatial profiles are obtained by averaging across the direction normal to the growth direction (z).

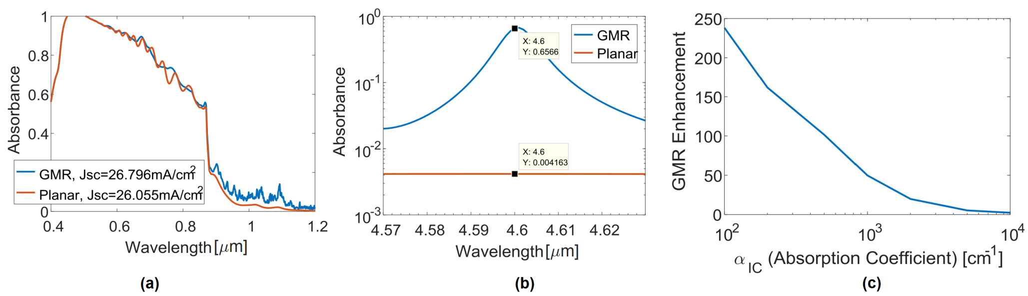

Fig. 3. Calculated absorbance spectrum (a) at $\lambda = 0.4 - 1.2\,\mu$m (GaAs and QD interband transitions) and (b) around $\lambda = 4.6\,\mu$m (QD intraband optical transition) under AM1.5G illumination. (c) GMR Enhancement as a function of the QD intraband optical absorption (α_{IC}) at $\lambda = 4.6\,\mu$m.

2. A. Luque, A. Martí, and C. Stanley, "Understanding intermediate-band solar cells," Nature Photonics **6**, 146–152 (2012).
3. A. Mellor, A. Luque, I. Tobías, and A. Martí, "The feasibility of high-efficiency inas/gaas quantum dot intermediate band solar cells," Solar Energy Materials and Solar Cells **130**, 225–233 (2014).
4. F. Cappelluti, G. Ghione, M. Gioannini, G. Bauhuis, P. Mulder, J. Schermer, M. Cimino, G. Gervasio, G. Bissels, E. Katsia *et al.*, "Novel concepts for high-efficiency lightweight space solar cells," in "E3S Web of Conferences," , vol. 16 (EDP Sciences, 2017), vol. 16, p. 03007.
5. B. L. Smith, M. A. Slocum, Z. S. Bittner, Y. Dai, G. T. Nelson, S. D. Hellstroem, R. Tatavarti, and S. M. Hubbard, "Inverted growth evaluation for epitaxial lift off (elo) quantum dot solar cell and enhanced absorption by back surface texturing," in "2016 IEEE 43rd Photovoltaic Specialists Conference (PVSC)," (2016), pp. 1276–1281.
6. F. Cappelluti, A. P. Cedola, A. Khalili, F. Elsehrawy, G. Bauhuis, P. Mulder, J. Schermer, G. Bissels, T. Aho, T. Niemi, M. Guina, D. Kim, J. Wu, and H. Liu, "Enabling high-efficiency inas/gaas quantum dot solar cells by epitaxial lift-off and light management," in "2017 IEEE 44th Photovoltaic Specialists Conference (PVSC)," (2017), p. to be published.
7. T. Khaleque and R. Magnusson, "Light management through guided-mode resonances in thin-film silicon solar cells," Journal of Nanophotonics **8**, 083,995–083,995 (2014).
8. A. Musu, F. Cappelluti, T. Aho, V. Polojärvi, T. K. Niemi, and M. Guina, "Nanostructures for light management in thin-film gaas quantum dot solar cells," in "Light, Energy and the Environment," (OSA, 2016), p. JW4A.45.
9. Y. Harada, T. Maeda, and T. Kita, "Intraband carrier dynamics in inas/gaas quantum dots stimulated by bound-to-continuum excitation," JAP **113**, 223,511 (2013).